Enhanced potency of aggregation inhibitors mediated by liquid condensates

Thomas C. T. Michaels[1,2] L. Mahadevan[3,4,*] and Christoph A. Weber[5,†]

[1]*Department of Biology, Institute of Biochemistry, ETH Zurich, Otto Stern Weg 3, 8093 Zurich, Switzerland*

[2]*Bringing Materials to Life Initiative, ETH Zurich, Switzerland*

[3]*Paulson School of Engineering and Applied Science, Harvard University, Cambridge, Massachusetts 02138, USA*

[4]*Department of Physics and Department of Organismic and Evolutionary Biology, Harvard University, Cambridge, Massachusetts 02138, USA*

[5]*Institute of Physics, Faculty of Mathematics, Natural Sciences, and Materials Engineering, University of Augsburg, Universitätsstraße 1, 86159 Augsburg, Germany*

(Received 7 May 2021; accepted 18 August 2022; published 8 December 2022)

Liquid condensates are membraneless organelles that form via phase separation in living cells. These condensates provide unique heterogeneous environments that have much potential in regulating a range of biochemical processes from gene expression to filamentous protein aggregation—a process linked to Alzheimer's and Parkinson's diseases. Here we theoretically study the physical interplay between protein aggregation, its inhibition, and liquid-liquid phase separation. Our key finding is that the action of protein aggregation inhibitors can be strongly enhanced by liquid condensates. The physical mechanism of this enhancement relies on the partitioning and colocalization of inhibitors with their targets inside the liquid condensate. Our theory uncovers how the physicochemical properties of condensates can be used to modulate inhibitor potency, and we provide experimentally testable conditions under which drug potency is maximal. Our findings suggest design principles for protein aggregation inhibitors with respect to their phase-separation properties.

DOI: 10.1103/PhysRevResearch.4.043173

I. INTRODUCTION

The proteostasis network in living cells uses chaperones as key players for protein quality control [1,2]. The main role of chaperones is to stabilize the native fold of proteins, but they are also involved in degradation processes such as lysosome-mediated degradation of dysfunctional proteins [3,4]. A decline of the proteostasis network, due to ageing, for example [2], causes the accumulation of misfolded proteins and their subsequent aggregation into filamentous aggregates and amyloid fibrils—a process linked to over 50 devastating disorders, including Alzheimer's and Parkinson's diseases [5–9]. It is therefore important to obtain insights into the mechanisms underlying filamentous protein aggregation.

These mechanistic insights are particularly important for understanding how inhibitors affect protein aggregation. A range of compounds, including molecular chaperones [10] or rationally designed inhibitors, such as small druglike molecules [11,12], nanoparticles [13], and antibodies [14], have been shown to affect aggregation *in vitro* and *in vivo* [11–27]. Recent *in vitro* studies indicate that these compounds inhibit aggregation by binding to specific targets, including monomers, aggregate growth ends, or surfaces [10,28–31]. However, these different inhibition mechanisms have been elucidated in homogeneous *in vitro* systems, disregarding that cells are spatially heterogeneous due to the presence of organelles.

A new class of organelles that has recently received significant attention are protein condensates. They form via phase separation from the cyto- or nucleoplasm and share most physical properties with liquid-like, condensed droplets [32–35]. Liquid condensates provide physicochemical environments distinct from the surrounding cytoplasm and nucleoplasm, allowing a range of biochemical reactions associated with biological function or dysfunction to be spatially regulated. Recent experimental [35–37] and theoretical [38] studies show that condensates can affect amyloid aggregation. For example, stress granules concentrate monomers causing aggregation to occur only inside the condensates [39,40]. Condensates can accumulate chaperones capable of either suppressing aberrant phase transition of condensates [41] or driving amyloid formation by sequestering misfolded proteins [42–44]. Chaperones are also involved in the control of condensate stability [45] and the surveillance of stress granule quality [46,47].

The relevance of liquid condensates for the spatial organization of chaperones and filamentous aggregates suggests that spatial compartmentalization may play an important role in regulating and suppressing protein aggregation. Similarly, the action of synthetic aggregation inhibitors may be affected by the presence of liquid condensates. Abbreviating

*lmahadev@g.harvard.edu

†christoph.weber@physik.uni-augsburg.de

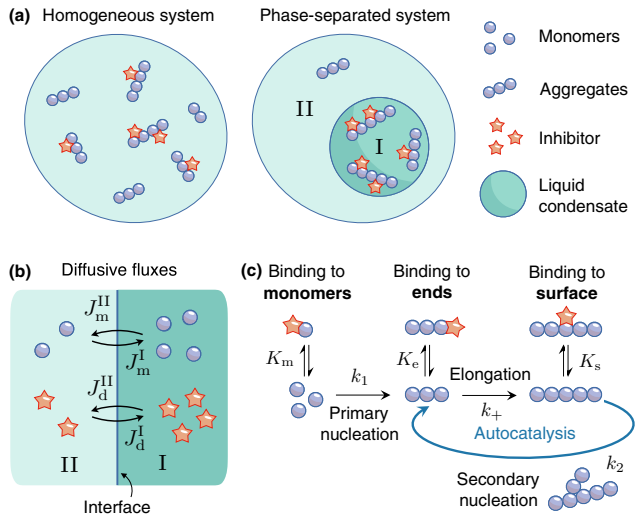

FIG. 1. How liquid-like condensates impact protein aggregation inhibition. (a) We determine the physical conditions when the presence of a phase-separated condensate (phase I, right) yields a higher degree of inhibition of aggregation (e.g., fewer aggregates at the end of the reaction) compared with a homogeneous system (left). (b) Definition of partitioning of monomers and drug components and associated nonequilibrium diffusive fluxes across the condensate interface. We neglect diffusive exchange of aggregates through the interface. (c) The reaction network of filamentous protein aggregation and three established mechanisms of inhibition [10,28–30].

both chaperones and synthetic inhibitors as "drugs," we raise the following question: How do liquid condensates affect drug-mediated inhibition of protein aggregation [Fig. 1(a)]? Here, we address this question by presenting a physical model of protein aggregation inhibition coupled to liquid-liquid phase separation. We find that liquid condensates can significantly amplify drug-mediated inhibition of protein aggregation. The mechanism for this amplification builds on the colocalization inside the condensate of the inhibiting drug and its target [Fig. 1(a)]. The key control parameters are the volume of the condensate and the partitioning coefficients of drug and monomers. Our results reveal a simple physical mechanism that may allow liquid condensates to control protein aggregation in cells and are likely to inspire new drug discovery strategies against protein aggregation disorders that could improve drug efficacy.

II. AGGREGATION KINETICS WITH INHIBITORS AND LIQUID CONDENSATES

We consider a system of volume V containing a phase-separated liquid-like condensate of volume V^{I} (phase I) coexisting with the surrounding, dilute phase (phase II). Phase I is rich in some protein A, while phase II is dilute in A but is rich in another protein, lipids, or water, shortly denoted as the B component [Fig. 1(a)]. In addition to the phase-separating components A and B the system contains a concentration $M_{\mathrm{m}}^{\mathrm{tot}}$ of monomeric protein and a concentration c_{d} of an inhibitor of aggregation. We assume that all aggregating species and the drug are sufficiently dilute with respect to A and B such that their impact on AB-phase separation can be neglected (see Supplemental Material [48] Sec. 1.3.1). The coexisting phases I and II thus create distinct biochemical environments for aggregation and can give rise to diffusive fluxes across the interface that partition aggregating monomers and drug components, which we denote with i (i.e., i denotes monomers or inhibitors). By equating chemical potentials of component i between the two phases, we can calculate the equilibrium partitioning coefficient of species i as $p_i = c_i^{\mathrm{I}}|_{\mathrm{eq}}/c_i^{\mathrm{II}}|_{\mathrm{eq}}$. Here, c_i^{I} and c_i^{II} are the concentrations of component i in phases I and II, respectively. p_i is determined by the degree of phase separation and the relative strength of interaction between species i and A or B (see Supplemental Material [48] Sec. 1.3.1 and Ref. [38]). Favoring interactions between i and A, for instance, leads to $p_i > 1$, i.e., enrichment of i in the condensate. Deviations from partitioning equilibrium lead to interphase fluxes of species i that reestablish equilibrium [Fig. 1(b)]. For small deviations from equilibrium, these fluxes depend linearly on the concentrations in phases I and II (see Supplemental Material [48] Sec. S1.3.2 and Ref. [38])

$$J_i^{\mathrm{I}} = -J_i^{\mathrm{II}} = -k_{\mathrm{diff},i}\left(c_i^{\mathrm{I}} - p_i\, c_i^{\mathrm{II}}\right), \tag{1a}$$

where p_i is the equilibrium partitioning coefficient and $k_{\mathrm{diff},i} = 4\pi R D_i$ is the relaxation rate toward equilibrium, with R being the radius of the condensate and D being the diffusion coefficient of species i. Note that these fluxes vanish at partitioning equilibrium, i.e., when $c_i^{\mathrm{I}}/c_i^{\mathrm{II}} = p_i$.

In the presence of a liquid condensate, aggregation occurs in both phase I and phase II involving a number of different microscopic events [49–56], which are illustrated in Fig. 1(c). Aggregation is initiated by primary nucleation, i.e., the formation of the smallest aggregates directly from the monomers. Aggregates then grow by elongation. In addition, aggregation is often accelerated by secondary nucleation mechanisms [57], including fragmentation, lateral branching, or surface-catalyzed secondary nucleation [Fig. 1(c)]. These secondary nucleation processes are in general characterized by a dependence on the current population of aggregates and introduce therefore an autocatalytic cycle in the system [Fig. 1(c)].

We focus here on suppression of aggregation by the inhibitor through three established mechanisms [10,28–30], including inhibitor binding to (i) free monomers, (ii) aggregate growth ends, and (iii) aggregate surface sites, as depicted in Fig. 1(c) (see Supplemental Material [48] Fig. S1 for examples of inhibitors). For simplicity, we neglect drug binding to other species, including intermediate oligomers, but note that our framework can in principle be generalized to account for these inhibition mechanisms.

To couple the aggregation kinetics with liquid-liquid phase separation, we consider an approximate case where the partitioning of monomers and inhibitors is close to equilibrium at all times. This approximation is valid if these species diffuse fast compared with the characteristic timescales of aggregation and inhibitor binding (see Supplemental Material [48] Sec. S1.4). Typical values for the aggregation rates and condensate sizes suggest that our approximation is consistent with experimental conditions (see Supplemental Material [48] Table S1). For simplicity, we restrict ourselves to monomers and drug molecules diffusing through the condensate interface

and neglect the diffusive exchange of aggregates. Aggregate diffusion is slow due to their large molecular weight, which limits their diffusion via slow reptation in an environment of entangled filaments. Under these assumptions, deviations from the equilibrium partitioning, caused by slow aggregation, are quasistatically balanced by rapid diffusive fluxes of monomers and drug molecules across the condensate interface [Eq. (1a)]. These fluxes ensure that the partitioning of the respective species stays approximately close to equilibrium at all times. Moreover, as suggested by recent inhibition experiments *in vitro* [10], inhibitor binding to its target is often much faster than aggregation, such that this binding kinetics can be considered to be in pre-equilibrium (see Supplemental Material [48] Sec. S2 and Table S1). In this case we can capture the impact of the drug on aggregation by means of effective rate parameters (see Supplemental Material [48] Secs. S1.2 and S1.3).

$$k_1\big(c_\mathrm{d}^{(\alpha)}\big) = k_1\left(\frac{1}{1+K_\mathrm{m}c_\mathrm{d}^{(\alpha)}}\right)^{n_1}, \tag{1b}$$

$$k_2\big(c_\mathrm{d}^{(\alpha)}\big) = k_2\left(\frac{1}{1+K_\mathrm{m}c_\mathrm{d}^{(\alpha)}}\right)^{n_2}\left(\frac{1}{1+K_\mathrm{s}c_\mathrm{d}^{(\alpha)}}\right), \tag{1c}$$

$$k_+\big(c_\mathrm{d}^{(\alpha)}\big) = k_+\left(\frac{1}{1+K_\mathrm{m}c_\mathrm{d}^{(\alpha)}}\right)\left(\frac{1}{1+K_\mathrm{e}c_\mathrm{d}^{(\alpha)}}\right), \tag{1d}$$

where k_1, k_2, and k_+ denote the aggregation rate constants for primary nucleation, secondary nucleation, and growth in the absence of the inhibitor and K_i are the equilibrium binding constants of the drug to monomers ($i = \mathrm{m}$), fibril ends ($i = \mathrm{e}$), and fibril surface sites ($i = \mathrm{s}$).

By combining the above ingredients, a coupled set of kinetic equations describing inhibited aggregation in both phases $\alpha = \mathrm{I}, \mathrm{II}$ can be written as (see Supplemental Material [48] Sec. S2)

$$\frac{dc_\mathrm{a}^{(\alpha)}}{dt} = k_1\big(c_\mathrm{d}^{(\alpha)}\big)\big[M_\mathrm{m}^{(\alpha)}\big]^{n_1} + k_2\big(c_\mathrm{d}^{(\alpha)}\big)\big[M_\mathrm{m}^{(\alpha)}\big]^{n_2}M_\mathrm{a}^{(\alpha)}, \tag{1e}$$

$$\frac{dM_\mathrm{a}^{(\alpha)}}{dt} = 2k_+\big(c_\mathrm{d}^{(\alpha)}\big)M_\mathrm{m}^{(\alpha)}\,c_\mathrm{a}^{(\alpha)}, \tag{1f}$$

$$\frac{dM_\mathrm{m}^{(\alpha)}}{dt} = -2k_+\big(c_\mathrm{d}^{(\alpha)}\big)M_\mathrm{m}^{(\alpha)}\,c_\mathrm{a}^{(\alpha)} + \frac{J_\mathrm{m}^{(\alpha)}}{V^{(\alpha)}}, \tag{1g}$$

$$\frac{dc_\mathrm{d}^{(\alpha)}}{dt} = \frac{J_\mathrm{d}^{(\alpha)}}{V^{(\alpha)}}, \tag{1h}$$

where $c_\mathrm{a}^{(\alpha)}$ and $M_\mathrm{a}^{(\alpha)}$ denote the number and mass concentrations of aggregates, respectively, in phase α, and $M_\mathrm{m}^{(\alpha)}$ is the monomer concentration in phase α, and $c_\mathrm{d}^{(\alpha)}$ is the drug concentration in phase α. Equation (1e) describes the formation of new aggregates by primary and secondary nucleation, with n_1 and n_2 denoting the respective reaction orders. Depending on the value of n_2, the secondary nucleation rate describes different processes [56]: fragmentation ($n_2 = 0$), branching ($n_2 = 1$), and surface-catalyzed secondary nucleation ($n_2 > 1$) (see Supplemental Material [48] Fig. S1 for typical reaction orders). These reaction terms can be combined to describe the competition of multiple nucleation processes. Equation (1f) captures the buildup of aggregate mass by monomer pickup, where k_+ is the rate constant for elongation and the factor 2 accounts for two growing ends per aggregate. Equation (1g) accounts for monomer depletion by growth and the interphase flux maintaining the monomer equilibrium partitioning. Equation (1h) describes the partitioning dynamics of the drug.

The validity of Eqs. (1a)–(1h) relies on a few implicit assumptions. For example, phase coexistence and the aggregation kinetics are usually coupled since both are determined by the chemical potentials of the components [58]. However, for irreversible aggregation processes it can shown that both actually decouple [59]. Moreover, focusing on irreversible aggregation in Eqs. (1a)–(1h), we neglected the effect of monomer dissociation (inverse process of elongation) and filament coagulation (inverse process of fragmentation). These processes may be easily included in the kinetic equations [60–62]. However, for typical amyloid-forming systems their effect on the aggregate concentration is negligible except in the very late stages of aggregation, i.e., past the plateau phase when the aggregate size distribution slowly relaxes to thermodynamic equilibrium. Finally, we consider system and condensate volumes, V and V^I, to be sufficiently large (>1 pL) such that stochastic effects on primary nucleation are negligible [63].

Overall, our model has three aggregation rate parameters, reaction orders for primary and secondary nucleation, binding equilibrium constants for each inhibition mechanism, and three phase-separation parameters: compartment volume V^I, and the partitioning coefficients for drug and monomers, p_d and p_m. In the following, we will choose the aggregation parameters such that they are consistent with *in vitro* experiments [53] and vary the phase-separation parameters in ranges such that they are consistent with protein condensates found *in vitro* and *in vivo* (see Table I for a summary of parameters in the model and associated values).

III. RESULTS

A. Condensates enhance inhibition of secondary nucleation

To study the impact of a liquid condensate on aggregation inhibition, we numerically studied Eqs. (1a)–(1h) and determined asymptotic analytical solutions for the number and mass concentrations of aggregates inside and outside the liquid condensate (Fig. 2(a); see Supplemental Material [48] Sec. S2.5). As an illustrative example, we focus on the inhibition of secondary nucleation by drugs that bind to the surface of existing fibrils. In Figs. 2(a) and 2(b) we consider the uninhibited, homogeneous system (no condensates, no drug) as a reference and compare the number concentration of aggregates formed for three systems: (i) no condensates with drug, (ii) condensates, no drug, and (iii) condensates with drug; systems (i) and (iii) have the same total drug concentration. Strikingly, while in all three systems the terminal ($t \to \infty$) number concentration of aggregates is reduced relative to the reference, we see that the system with condensates and drugs is most effective in inhibiting aggregation. Moreover, adding the drug to a heterogeneous system results in a significantly more pronounced reduction compared with adding the same amount of drug to the homogeneous system [Fig. 2(b)]. Therefore the presence of liquid condensates can enhance the

TABLE I. List of parameters in kinetic model and values used for generating the graphs in Fig. 2. Note that in the limit of fast inhibitor binding and rapid establishment of phase equilibrium the exact values of the binding or unbinding and diffusion rates do not affect the plots in Fig. 2, as long as these rates are fast compared with aggregation.

Symbol	Meaning	Value
k_1	rate constant for primary nucleation	$10^{-4}\ \mathrm{M}^{-1}\ \mathrm{s}^{-1}$
k_2	rate constant for secondary nucleation	$4 \times 10^{4}\ \mathrm{M}^{-2}\ \mathrm{s}^{-1}$
k_+	rate constant for aggregate elongation (growth)	$3 \times 10^{6}\ \mathrm{M}^{-1}\ \mathrm{s}^{-1}$
n_1	reaction order for primary nucleation	2
n_2	reaction order for secondary nucleation	2
$M_{\mathrm{m}}^{\mathrm{tot}}$	total monomer concentration	1 μM
$c_{\mathrm{d}}^{\mathrm{tot}}$	total drug concentration	2 μM
$K_{D,i}$	binding constant for inhibitor binding to aggregate ends ($i = \mathrm{e}$), aggregate surface ($i = \mathrm{s}$), or monomers ($i = \mathrm{m}$)	$10^{6}\ \mathrm{M}^{-1}$ (for surface)
V^{I}/V	fraction of volume occupied by condensate	10^{-3}
p_{m}	monomer partition coefficient	20
p_{d}	drug partition coefficient	20

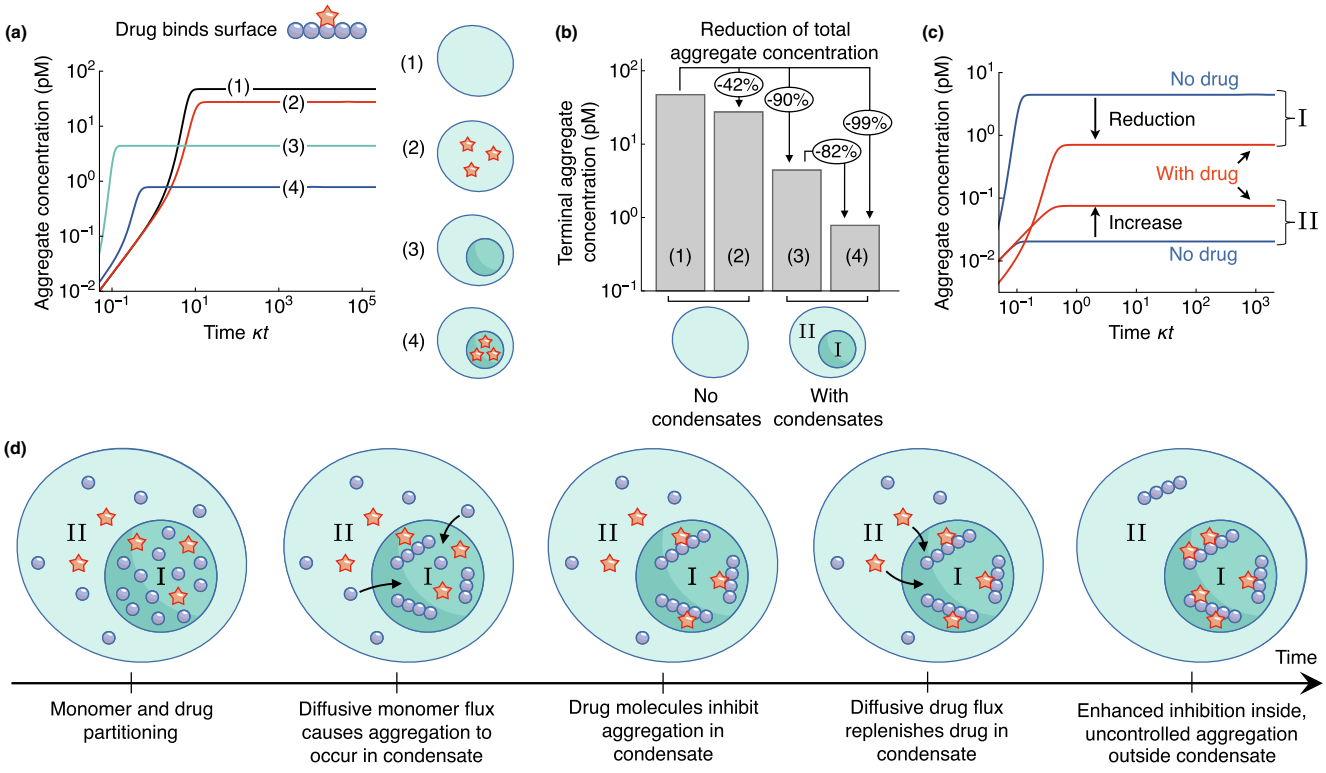

FIG. 2. Mechanism by which liquid condensates amplify inhibition of secondary nucleation. (a) Representative aggregation time courses for different systems (from top to bottom in terms of final plateau): (1) a homogeneous system without an inhibitor, (2) a homogeneous system with an inhibitor of secondary nucleation, (3) a heterogeneous system with a liquid condensate in the absence of the drug, and (4) same as system (3), but in the presence of the drug. A list of parameters used to generate the plots can be found in Table 1. (b) Number concentration of aggregates at the end of the aggregation reaction for the four systems [systems (1)–(4)] considered in (a). (c) Aggregation time course inside (phase I, top part of plot) and outside (phase II, bottom part of plot) the liquid condensate without and with the drug. We see that adding the drug causes a reduction of aggregate concentration inside the condensate (phase I) but leads to an increase in aggregate concentration outside the condensate (phase II). (d) Schematic representation of the positive feedback mechanism causing enhanced inhibition inside the liquid condensate. For $p_{\mathrm{m}} > 1$, aggregation occurs primarily in phase I due to the diffusive flux of monomers maintaining equilibrium. As drug molecules in phase I bind to their target ($p_{\mathrm{d}} > 1$), their concentration decreases. The resulting concentration imbalance across the condensate interface causes a diffusive flux of drug molecules from phase II to phase I to restore phase equilibrium. As a result, inhibition is enhanced inside the condensate (phase I), but the reaction proceeds in an uncontrolled fashion outside (phase II).

inhibitory action of the drug compared with the homogeneous system.

B. A positive feedback mechanism underlies enhanced inhibition in the presence of condensates

To understand the mechanism underlying this enhancement effect, we consider the impact of the drug on the aggregate concentration inside (phase I) and outside (phase II) the condensate [Fig. 2(c)]. We find that, while the drug inhibits aggregation in phase I, aggregation in phase II yields more aggregates in the presence of the drug compared with not having the drug. This counterintuitive effect is a direct consequence of the rapid tendency of monomers and drug components to reestablish partitioning equilibrium [Fig. 2(d)]. Consider the case where monomers and drugs partition preferentially into the condensate ($p_m > 1$, $p_d > 1$). Because $p_m > 1$, aggregation in phase I is accelerated compared with the continuous phase II [38]. As aggregation occurs in phase I, further monomers diffuse from phase II to phase I to maintain the monomer partitioning equilibrium, causing aggregation to occur primarily in phase I [38]. Partitioning of inhibitors into the condensate then leads to an increase in binding events of drug molecules to the aggregates inside the condensate. Therefore further drug molecules diffuse from the outside into the condensate to maintain the chemical potential of inhibitors constant across the interface of the condensate. This positive feedback in phase I couples to negative feedback in phase II, where drug molecules are continuously depleted in favor of the condensate. As a result, aggregation in phase I is suppressed, while aggregation in phase II potentially remains "uncontrolled" due to positive feedback. In other words, inhibition is enhanced in phase I, while it is lowered in phase II.

C. Physical conditions for enhanced inhibition of secondary nucleation by condensates

To understand which of these competing effects dominate, we need to quantify how the phase-separation parameters of volume and partitioning coefficients affect the total amount of aggregates in the system. To this end, we introduce an enhancement function $\mathcal{E}$ as

$$\mathcal{E} = \frac{c_a(\infty)|_{\text{homo}}}{\bar{c}_a(\infty)}. \tag{2a}$$

The enhancement $\mathcal{E}$ compares the final aggregate concentration formed in a homogeneous system in the presence of the drug, $c_a(\infty)|_{\text{homo}}$, with the average aggregate concentration formed with the same amount of drug in the phase-separated system (see Supplemental Material [48] Sec. S3):

$$\bar{c}_a(\infty) = \frac{V^I}{V} c_a^I(\infty) + \frac{V - V^I}{V} c_a^{II}(\infty). \tag{2b}$$

For $\mathcal{E} > 1$, the condensate enhances inhibition in the entire system compared with a homogeneous solution. For large condensates ($V^I \simeq V$), we find that inhibition is enhanced for $p_d \gg 1$. For $p_d \ll 1$, we find $\mathcal{E} < 1$, i.e., the phase-separated system yields more aggregates than the homogeneous one. Enhanced inhibition therefore occurs if both the inhibitor and the target are concentrated inside the condensate (colocalization). For small condensates ($V^I \ll V$), the contribution of $c_a^I(\infty)$ to the average concentration $\bar{c}_a(\infty)$ is reduced, making the system more susceptible to uncontrolled aggregation in phase II. Thus, in the limit of small condensates, the drug should preferably partition outside the condensate ($p_d \ll 1$). Overall, our results suggest that that there are two competing effects at play: Effective enhancement of inhibition by the condensate requires colocalization of the drug with the aggregates inside the condensate while avoiding uncontrolled aggregation outside. Consistently, the drug should partition in phase I for large condensates, while for smaller droplets the drug should suppress aggregation outside the condensate.

D. Optimal enhancement

This qualitative change of mechanism with condensate volume raises the question of which system yields the most effective reduction of aggregate concentration. To this end, we compare the terminal aggregate concentrations for different values of drug partitioning p_d and condensate volumes V^I/V and for the different systems [Fig. 3(b)]: (i) no condensates with drug, (ii) condensates, no drug, and (iii) condensates with drug. For large condensates the optimal system depends on p_d. When $p_d \ll 1$, the optimal choice is to add the drug to a homogeneous solution, while if the drug is enriched in the condensate ($p_d \gg 1$), the most effective suppression of aggregation occurs in the phase-separated system in the presence of the drug. For intermediate condensate volumes, adding the drug to the heterogeneous system is the best strategy for all values of p_d. By contrast, for smaller condensates, adding the drug to the phase-separated system causes an *increase* in the overall aggregate concentration due to uncontrolled aggregation in phase II. In this case, the optimal solution is the phase-separated system without the drug. The resulting phase diagram, shown in Fig. 3(c), thus provides a practical strategy for choosing the most effective system to suppress aggregation depending on the phase-separation parameters.

E. Condensates increase potency of aggregation inhibitors

Our theory predicts under which conditions condensates promote the activity of protein aggregation inhibitors relative to a homogeneous system. This implies that an equivalent degree of inhibition compared with the homogeneous system can be realized using a smaller amount of drug in the presence of condensates. In other words, liquid condensates can enhance the potency of a drug. To illustrate this effect, we define for both the homogeneous and the phase-separated system a drug-response curve $\mathcal{R}(c_d)$ given as the relative difference between asymptotic fibril concentrations with and without drug, $\mathcal{R}(c_d) = 1 - \bar{c}_a(\infty)/\bar{c}_a(\infty)|_{c_d=0}$ [Fig. 4(a)]. On the basis of the response function, we introduce the drug potency $\mathcal{P} = 1/\text{EC}_{50}$ as the inverse of the drug concentration necessary to suppress 50% of the aggregates, denoted as EC_{50}. The smaller EC_{50} is, the more potent is the drug. In Fig. 4(b), we show the relative potency, defined as the ratio between the EC_{50} values in the absence and in the presence of condensates, respectively (see Supplemental Material [48] Sec. S4). We see that the relative potency increases with decreasing drop

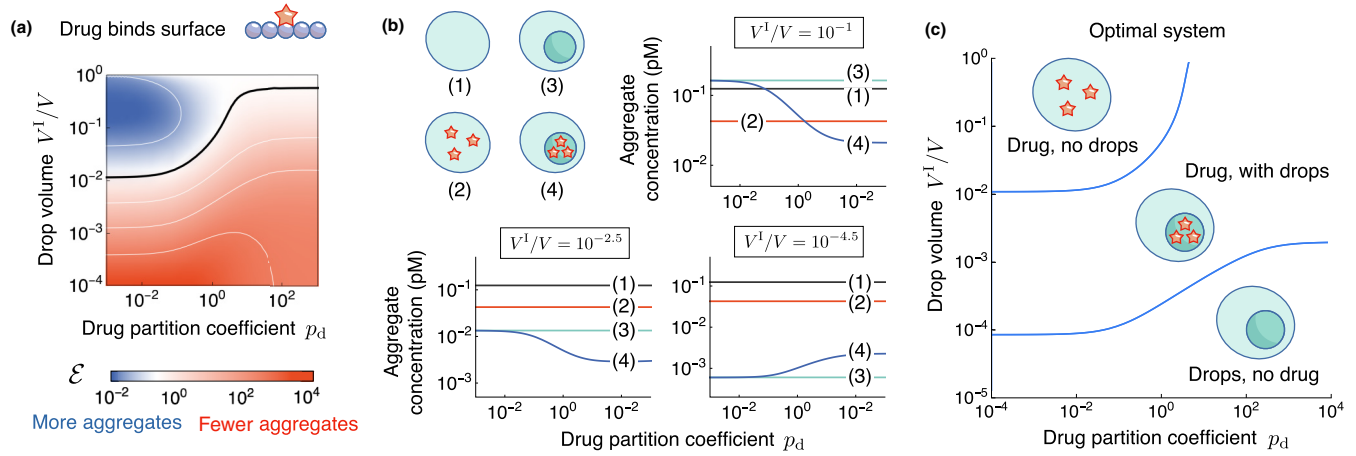

FIG. 3. Conditions for enhanced inhibition and phase diagram of optimal system. (a) Enhancement function $\mathcal{E} = c_{\mathrm{a}}(\infty)|_{\mathrm{homo}}/\overline{c}_{\mathrm{a}}(\infty)$ against drop volume V^{I}/V and drug partitioning p_{d} (for fixed p_{m} and drug concentration). We separate regions where liquid droplets enhance ($\mathcal{E} > 1$, red) or reduce ($\mathcal{E} < 1$, blue) the effect of an inhibitor of secondary nucleation. Contour lines for $\mathcal{E}$ are shown in logarithmic scale in steps of $10^{0.5}$. (b) Comparison of terminal number concentration of aggregates formed for different systems [(1) no condensates, (2) no condensates + drug, (3) condensates, (4) condensates + drug] against drug partitioning p_{d}. The plots are shown for $V^{\mathrm{I}}/V = 10^{-1}$ (top right), $V^{\mathrm{I}}/V = 10^{-2.5}$ (bottom left), and $V^{\mathrm{I}}/V = 10^{-4.5}$ (bottom right). (c) Phase diagram indicating the system that yields the most effective reduction of total aggregate concentration depending on V^{I}/V and p_{d} for an inhibitor of secondary nucleation.

volume in the limit of large condensates. In this limit, we find

$$\mathcal{P}_{\mathrm{rel}} = \frac{\mathrm{EC}_{50}|_{\mathrm{homo}}}{\mathrm{EC}_{50}|_{\mathrm{drops}}} \simeq \frac{p_{\mathrm{d}}}{1 + (p_{\mathrm{d}} - 1)V^{\mathrm{I}}/V}. \tag{3}$$

The relative potency $\mathcal{P}_{\mathrm{rel}}$ increases from unity for large condensates to a value equal to the drug partitioning p_{d} when the condensate volume is decreased. Hence reducing the volume of the condensate V^{I}/V and/or increasing the drug enrichment factor p_{d} lead to a strong increase in the relative potency. This increase corresponds to a strong reduction of the amount of drug necessary to inhibit aggregation. For small condensates, the optimal system becomes the phase-separated system without drug [Fig. 3(c)]; correspondingly, the potency decreases due to uncontrolled aggregation in phase II.

IV. DISCUSSION AND CONCLUSIONS

Heterogeneous environments have much potential in regulating biochemical reactions [32–35]. Our present study shows that liquid-like condensates can strongly affect drug-mediated inhibition of filamentous protein aggregation by providing such a heterogeneous environment composed of two coexisting phases. A key finding is that the potency of

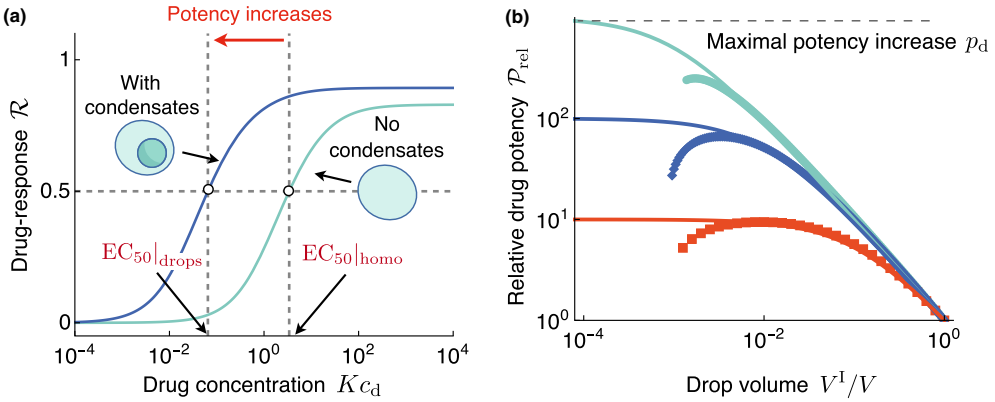

FIG. 4. Liquid condensates increase the potency of protein aggregation inhibitors. (a) Drug-response curve $\mathcal{R}(c_{\mathrm{d}})$ in the absence and in the presence of a liquid condensate. The presence of the liquid condensate increases the potency by reducing EC_{50}. The plot is shown for an inhibitor of secondary nucleation using the same parameters as in Fig. 3(c) except for $p_{\mathrm{d}} = 10^2$ and $V^{\mathrm{I}}/V = 10^{-2}$. (b) Relative drug potency $\mathcal{P}_{\mathrm{rel}}$ of inhibitors that bind to fibril surfaces against drop volume for $p_{\mathrm{d}} = 10$ (plotted at bottom of graph), $p_{\mathrm{d}} = 10^2$ (plotted in middle of graph), and $p_{\mathrm{d}} = 10^3$ (plotted at top of graph). The potency is defined as $\mathcal{P} = 1/\mathrm{EC}_{50}$ of the respective system. For small condensates, the potency of the inhibitor of secondary nucleation decreases due to uncontrolled aggregation in phase II. The solid lines indicate Eq. (3).

inhibitors can be increased due to the presence of a liquid condensate. This increase in potency implies that a significantly smaller drug dose is required to equally inhibit aggregation compared with the corresponding homogeneous system. We find that this potency increase depends on the colocalization of the inhibitor with its target within the liquid condensate leading to a positive feedback on the inhibition of aggregates. In a Flory-Huggins model of phase separation, we can calculate the degree of drug or monomer partitioning in the dilute limit (see Supplemental Material [48] Eq. (S12)). The partitioning of species i depends on parameters such as the degree of phase separation, molecular volumes, and the relative interaction parameter between species i and the phase-separating components A and B, derived from multiple microscopic processes and specific interactions. These parameters may be tuned experimentally to affect the tendencies of inhibitors and aggregates to colocalize within the droplet phase.

To experimentally scrutinize our key findings, we propose considering protein-rich condensates which recruit aggregation-prone monomers as well as aggregation inhibitors (chaperones or synthetic drugs that are both dilute compared to the condensate components, and determining the response as a function of inhibitor concentration with and without condensates [Fig. 4(a)].

In living cells, the colocalization of inhibitors and aggregates may not only increase the therapeutic outcome but also reduce the toxic effects on the organism by preventing drug molecules from interacting with other sensitive cellular domains. Thus our finding of an enhanced drug potency due to the presence of condensates suggests revisiting nominally efficacious drugs that have been disregarded in a homogeneous setting due to their high toxicity and shifting the focus to how drugs act specifically in the context of a spatially organized, intracellular environment.

ACKNOWLEDGMENTS

We thank Sudarshana Laha for valuable feedback on the Supplemental Material. We also thank Simon Alberti, Titus Franzmann, and Paolo Arosio, for very helpful comments on the manuscript. TCTM acknowledges support from the Swiss National Science Foundation and Peterhouse, Cambridge. We also thank the visitor program of the Max Planck Institute for the Physics of Complex Systems for hosting T.C.T.M. and providing a stimulating research environment. C.A.W. acknowledges the European Research Council (ERC) under the European Union's Horizon 2020 research and innovation program ("Fuelled Life" with Grant Agreement No. 949021) for financial support.

[1] R. I. Morimoto and A. M. Cuervo, Protein homeostasis and aging: taking care of proteins from the cradle to the grave, J. Gerontol., Ser. A **64A**, 167 (2009).

[2] M. S. Hipp, P. Kasturi, and F. U. Hartl, The proteostasis network and its decline in ageing, Nat. Rev. Mol. Cell Biol. **20**, 421 (2019).

[3] E. R. P. Zuiderweg, L. E. Hightower, and J. E. Gestwicki, The remarkable multivalency of the Hsp70 chaperones, Cell Stress Chaperones **22**, 173 (2017).

[4] R. Donev, *Molecular Chaperones in Human Disorders*, Advances in Protein Chemistry and Structural Biology Vol. 114 (Academic, New York, 2019).

[5] T. P. J. Knowles, M. Vendruscolo, and C. M. Dobson, The amyloid state and its association with protein misfolding diseases, Nat. Rev. Mol. Cell Biol. **15**, 384 (2014).

[6] F. Chiti and C. M. Dobson, Protein misfolding, functional amyloid, and human disease, Annu. Rev. Biochem. **75**, 333 (2006).

[7] C. M. Dobson, The amyloid phenomenon and its links with human disease, Cold Spring Harbor Perspect. Biol. **9**, a023648 (2017).

[8] C. M. Dobson, Protein folding and misfolding, Nature (London) **426**, 884 (2003).

[9] D. J. Selkoe and J. Hardy, The amyloid hypothesis of Alzheimer's disease at 25 years, EMBO Mol. Med. **8**, 595 (2016).

[10] P. Arosio, T. C. T. Michaels, S. Linse, C. Månsson, C. Emanuelsson, J. Presto, J. Johansson, M. Vendruscolo, C. M. Dobson, and T. P. J. Knowles, Kinetic analysis reveals the diversity of microscopic mechanisms through which molecular chaperones suppress amyloid formation, Nat. Commun. **7**, 10948 (2016).

[11] J. Habchi, P. Arosio, M. Perni, A. R. Costa, M. Yagi-Utsumi, P. Joshi, S. Chia, S. I. A. Cohen, M. B. D. Müller, S. Linse, E. A. A. Nollen, C. M. Dobson, T. P. J. Knowles, and M. Vendruscolo, An anticancer drug suppresses the primary nucleation reaction that initiates the production of the toxic Aβ42 aggregates linked with Alzheimer's disease, Sci. Adv. **2**, e1501244 (2016).

[12] Y. Sun, A. Kakinen, C. Zhang, Y. Yang, A. Faridi, T. P. Davis, W. Cao, P. C. Ke, and F. Ding, Amphiphilic surface chemistry of fullerenols is necessary for inhibiting the amyloid aggregation of alpha-synuclein NACore, Nanoscale **11**, 11933 (2019).

[13] R. Vacha, S. Linse, and M. Lund, Surface effects on aggregation kinetics of amyloidogenic peptides, J. Am. Chem. Soc. **136**, 11776 (2014).

[14] F. A. Aprile, P. Sormanni, M. Perni, P. Arosio, S. Linse, T. P. J. Knowles, C. M. Dobson, and M. Vendruscolo, Selective targeting of primary and secondary nucleation pathways in Aβ42 aggregation using a rational antibody scanning method, Sci. Adv. **3**, e1700488 (2017).

[15] P. J. Muchowski, G. Schaffar, A. Sittler, E. E. Wanker, M. K. Hayer-Hartl, and F. U. Hartl, Hsp70 and Hsp40 chaperones can inhibit self-assembly of polyglutamine proteins into amyloid-like fibrils, Proc. Natl. Acad. Sci. USA **97**, 7841 (2000).

[16] G. W. Jones and M. F. Tuite, Chaperoning prions: the cellular machinery for propagating an infectious protein? Bioessays **27**, 823 (2005).

[17] P. J. Muchowski and J. L. Wacker, Modulation of neurodegeneration by molecular chaperones, Nat. Rev. Neurosci. **6**, 11 (2005).

[18] W. E. Balch, R. I. Morimoto, A. Dillin, and J. W. Kelly, Adapting proteostasis for disease intervention, Science **319**, 916 (2008).

[19] S. Perrett and G. W. Jones, Insights into the mechanism of prion propagation, Curr. Opin. Struct. Biol. **18**, 52 (2008).

[20] H. Zhang, L. Q. Xu, and S. Perrett, Studying the effects of chaperones on amyloid fibril formation, Methods **53**, 285 (2011).

[21] B. Mannini, R. Cascella, M. Zampagni, M. van Waarde-Verhagen, S. Meehan, C. Roodveldt, S. Campioni, M. Boninsegna, A. Penco, A. Relini, H. H. Kampinga, C. M. Dobson, M. R. Wilson, C. Cecchi, and F. Chiti, Molecular mechanisms used by chaperones to reduce the toxicity of aberrant protein oligomers, Proc. Natl. Acad. Sci. USA **109**, 12479 (2012).

[22] C. Månsson, V. Kakkar, E. Monsellier, Y. Sourigues, J. Harmark, H. H. Kampinga, R. Melki, and C. Emanuelsson, DNAJB6 is a peptide-binding chaperone which can suppress amyloid fibrillation of polyglutamine peptides at substoichiometric molar ratios, Cell Stress Chaperones **19**, 227 (2014).

[23] K. R. Brandvold and R. I. Morimoto, The chemical biology of molecular chaperones–Implications for modulation of proteostasis, J. Mol. Biol. **427**, 2931 (2015).

[24] M. Sablón-Carrazana, I. Fernández, A. Bencomo, R. Lara-Martínez, S. Rivera-Marrero, G. Domínguez, R. Pérez-Perera, L. F. Jiménez-García, N. F. Altamirano-Bustamante, M. Diaz-Delgado, F. Vedrenne, L. Rivillas-Acevedo, K. Pasten-Hidalgo, M. de L. Segura-Valdez, S. Islas-Andrade, E. Garrido-Magaña, A. Perera-Pintado, A. Prats-Capote, C. Rodríguez-Tanty, and M. M. Altamirano-Bustamante, Drug development in conformational diseases: A novel family of chemical chaperones that bind and stabilise several polymorphic amyloid structures, PLoS One **10**, e0135292 (2015).

[25] D. Zuo, J. Subjeck, and X. Y. Wang, Unfolding the role of large heat shock proteins: New insights and therapeutic implications, Front. Immunol. **7**, 75 (2016).

[26] J. M. Webster, A. L. Darling, V. N. Uversky, and L. J. Blair, Small heat shock proteins, big impact on protein aggregation in neurodegenerative disease, Front. Pharmacol. **10**, 1047 (2019).

[27] A. Wentink, C. Nussbaum-Krammer, and B. Bukau, Modulation of amyloid states by molecular chaperones, Cold Spring Harbor Perspect. Biol. **11**, a033969 (2019).

[28] M. M. Dedmon, J. Christodoulou, M. R. Wilson, and C. M. Dobson, Heat shock protein 70 inhibits alpha-synuclein fibril formation via preferential binding to prefibrillar species, J. Biol. Chem. **280**, 14733 (2005).

[29] S. L. Shammas, C. A. Waudby, S. Wang, A. K. Buell, T. P. Knowles, H. Ecroyd, M. E. Welland, J. A. Carver, C. M. Dobson, and S. Meehan, Binding of the molecular chaperone αB-crystallin to Aβ amyloid fibrils inhibits fibril elongation, Biophys. J. **101**, 1681 (2011).

[30] S. I. A. Cohen, P. Arosio, J. Presto, F. R. Kurudenkandy, H. Biverstål, L. Dolfe, C. Dunning, X. Yang, B. Frohm, M. Vendruscolo, J. Johansson, C. M. Dobson, A. Fisahn, T. P. J. Knowles, and S. Linse, A molecular chaperone breaks the catalytic cycle that generates toxic Aβ oligomers, Nat. Struct. Mol. Biol. **22**, 207 (2015).

[31] T. C. T. Michaels, C. A. Weber, and L. Mahadevan, Optimal control strategies for inhibition of protein aggregation, Proc. Natl. Acad. Sci. USA **116**, 14593 (2019).

[32] A. A. Hyman, C. A. Weber, and F. Jülicher, Liquid-liquid phase separation in biology, Annu. Rev. Cell Dev. Biol. **30**, 39 (2014).

[33] S. F. Banani, H. O. Lee, A. A. Hyman, and M. K. Rosen, Biomolecular condensates: organizers of cellular biochemistry, Nat. Rev. Mol. Cell Biol. **18**, 285 (2017).

[34] S. Alberti, A. Gladfelter, and T. Mittag, Considerations and challenges in studying liquid-liquid phase separation and biomolecular condensates, Cell **176**, 419 (2019).

[35] Y. Shin and C. P. Brangwynne, Liquid phase condensation in cell physiology and disease, Science **357**, eaaf4382 (2017).

[36] S. Alberti and A. A. Hyman, Are aberrant phase transitions a driver of cellular aging?, BioEssays **38**, 959 (2016).

[37] L. Malinovska, S. Kroschwald, and S. Alberti, Protein disorder, prion propensities, and self-organizing macromolecular collectives, Biochim. Biophys. Acta, Proteins Proteomics **1834**, 918 (2013).

[38] C. Weber, T. Michaels, and L. Mahadevan, Spatial control of irreversible protein aggregation, eLife **8**, e42315 (2019).

[39] A. Molliex, J. Temirov, J. Lee, M. Coughlin, A. P. Kanagaraj, H. J. Kim, T. Mittag, and J. P. Taylor, Phase separation by low complexity domains promotes stress granule assembly and drives pathological fibrillization, Cell **163**, 123 (2015).

[40] A. Patel, H. O. Lee, L. Jawerth, S. Maharana, M. Jahnel, M. Y. Hein, S. Stoynov, J. Mahamid, S. Saha, T. M. Franzmann, A. Pozniakovski, I. Poser, N. Maghelli, L. A. Royer, M. Weigert, E. W. Myers, S. Grill, D. Drechsel, A. A. Hyman, and S. Alberti, A liquid-to-solid phase transition of the ALS protein FUS accelerated by disease mutation, Cell **162**, 1066 (2015).

[41] D. Mateju, T. M. Franzmann, A. Patel, A. Kopach, E. E. Boczek, S. Maharana, H. O. Lee, S. Carra, A. A. Hyman, and S. Alberti, An aberrant phase transition of stress granules triggered by misfolded protein and prevented by chaperone function, EMBO J. **36**, 1669 (2017).

[42] T. Grousl, S. Ungelenk, S. Miller, C.-T. Ho, M. Khokhrina, M. P. Mayer, B. Bukau, and A. Mogk, A prion-like domain in Hsp42 drives chaperone-facilitated aggregation of misfolded proteins, J. Cell Biol. **217**, 1269 (2018).

[43] S. Specht, S. B. M. Miller, A. Mogk, and B. Bukau, Hsp42 is required for sequestration of protein aggregates into deposition sites in Saccharomyces cerevisiae, J. Cell Biol. **195**, 617 (2011).

[44] E. E. Boczek and S. Alberti, One domain fits all: Using disordered regions to sequester misfolded proteins, J. Cell Biol. **217**, 1173 (2018).

[45] S. Alberti, D. Mateju, L. Mediani, and S. Carra, Granulostasis: protein quality control of RNP granules, Front. Mol. Neurosci. **10**, 84 (2017).

[46] M. Ganassi, D. Mateju, I. Bigi, L. Mediani, I. Poser, H. O. Lee, S. J. Seguin, F. F. Morelli, J. Vinet, G. Leo, O. Pansarasa, C. Cereda, A. Poletti, S. Alberti, and S. Carra, A surveillance function of the HSPB8-BAG3-HSP70 chaperone complex ensures stress granule integrity and dynamism, Mol. Cell **63**, 796 (2016).

[47] S. Alberti and S. Carra, Quality control of membraneless organelles, J. Mol. Biol. **430**, 4711 (2018).

[48] See Supplemental Material at http://link.aps.org/supplemental/10.1103/PhysRevResearch.4.043173 for further details on the mathematical model.

[49] F. Oosawa and S. Asakura, *Thermodynamics of the Polymerization of Protein* (Academic, New York, 1975).

[50] T. P. J. Knowles, C. A. Waudby, G. L. Devlin, S. I. A. Cohen, A. Aguzzi, M. Vendruscolo, E. M. Terentjev, M. E. Welland, and C. M. Dobson, An analytical solution to the kinetics of breakable filament assembly, Science **326**, 1533 (2009).

[51] G. Ramachandran and J. B. Udgaonkar, Evidence for the existence of a secondary pathway for fibril growth during the aggregation of tau, J. Mol. Biol. **421**, 296 (2012).

[52] A. M. Ruschak and A. D. Miranker, Fiber-dependent amyloid formation as catalysis of an existing reaction pathway, Proc. Natl. Acad. Sci. USA **104**, 12341 (2007).

[53] S. I. A. Cohen, S. Linse, L. M. Luheshi, E. Hellstrand, D. A. White, L. Rajah, D. E. Otzen, M. Vendruscolo, C. M. Dobson, and T. P. J. Knowles, Proliferation of amyloid-β42 aggregates occurs through a secondary nucleation mechanism, Proc. Natl. Acad. Sci. USA **110**, 9758 (2013).

[54] A. Šarić, A. K. Buell, G. Meisl, T. C. T. Michaels, C. M. Dobson, S. Linse, T. P. J. Knowles, and D. Frenkel, Physical determinants of the self-replication of protein fibrils, Nat. Phys. **12**, 874 (2016).

[55] F. A. Ferrone, J. Hofrichter, and W. A. Eaton, Kinetics of sickle hemoglobin polymerization: II. A double nucleation mechanism, J. Mol. Biol. **183**, 611 (1985).

[56] T. C. T. Michaels, A. Šarić, J. Habchi, S. Chia, G. Meisl, M. Vendruscolo, C. M. Dobson, and T. P. J. Knowles, Chemical kinetics for bridging molecular mechanisms and macroscopic measurements of amyloid fibril formation, Annu. Rev. Phys. Chem. **69**, 273 (2018).

[57] M. Törnquist, T. C. T. Michaels, K. Sanagavarapu, X. Yang, G. Meisl, S. I. A. Cohen, T. P. J. Knowles, and S. Linse, Secondary nucleation in amyloid formation, Chem. Commun. **54**, 8667 (2018).

[58] J. Bauermann, S. Laha, P. M. McCall, F. Jülicher, and C. A. Weber, Chemical kinetics and mass action in coexisting phases, J. Am. Chem. Soc. **144**, 19294 (2022).

[59] W. Pönisch, T. C. T. Michaels, and C. A. Weber, Aggregation controlled by condensate rheology, Biophys. J. (2022).

[60] J. S. Schreck and J.-M. Yuan, A kinetic study of amyloid formation: Fibril growth and length distributions, J. Phys. Chem. B **117**, 6574 (2013).

[61] T. C. T. Michaels, G. A. Garcia, and T. P. J. Knowles, Asymptotic solutions of the Oosawa model for the length distribution of biofilaments, J. Chem. Phys. **140**, 194906 (2014).

[62] T. C. T. Michaels and T. P. J. Knowles, Role of filament annealing in the kinetics and thermodynamics of nucleated polymerization, J. Chem. Phys. **140**, 214904 (2014).

[63] T. C. T. Michaels, A. J. Dear, and T. P. J. Knowles, Stochastic calculus of protein filament formation under spatial confinement, New J. Phys. **20**, 055007 (2018).